ICln Ion Channel Splice Variants in *Caenorhabditis elegans*

VOLTAGE DEPENDENCE AND INTERACTION WITH AN OPERON PARTNER PROTEIN*

Johannes Fürst‡§, Markus Ritter‡§, Jakob Rudzki‡§, Johann Danzl‡, Martin Gschwentner‡, Elke Scandella‡¶, Martin Jakab‡, Matthias König‡, Bernhard Oehl‡, Florian Lang∥, Peter Deetjen‡, and Markus Paulmichl‡‡‡**

*From the ‡Department of Physiology, University of Innsbruck, Fritz-Pregl-Straße 3, A-6020 Innsbruck, Austria, the **Department of Physiology and Biochemistry, University of Milan, Via Celoria 26, I-20133 Milan, Italy, and the ∥Department of Physiology, University of Tübingen, Gmelinstraße 5, D-72076 Tübingen, Germany*

ICln is an ion channel identified by expression cloning using a cDNA library from Madin-Darby canine kidney cells. In all organisms tested so far, only one transcript for the ICln protein could be identified. Here we show that two splice variants of the ICln ion channel can be found in *Caenorhabditis elegans*. Moreover, we show that these two splice variants of the ICln channel protein, which we termed IClnN1 and IClnN2, can be functionally reconstituted and tested in an artificial lipid bilayer. In these experiments, the IClnN1-induced currents showed no voltage-dependent inactivation, whereas the IClnN2-induced currents fully inactivated at positive potentials. The molecular entity responsible for the voltage-dependent inactivation of IClnN2 is a cluster of positively charged amino acids encoded by exon 2a, which is absent in IClnN1. Our experiments suggest a mechanism of channel inactivation that is similar to the "ball and chain" model proposed for the *Shaker* potassium channel, *i.e.* a cluster of positively charged amino acids hinders ion permeation through the channel by a molecular and voltage-dependent interaction at the inner vestibulum of the pore. This hypothesis is supported by the finding that synthetic peptides with the same amino acid sequence as the positive cluster can transform the IClnN1-induced current to the current observed after reconstitution of IClnN2. Furthermore, we show that the nematode ICln gene is embedded in an operon harboring two additional genes, which we termed *Nx* and *Ny*. Co-reconstitution of Nx and IClnN2 and functional analysis of the related currents revealed a functional interaction between the two proteins, as evidenced by the fact that the IClnN2-induced current in the presence of Nx was no longer voltage-sensitive. The experiments described indicate that the genome organization in nematodes allows an effective approach for the identification of functional partner proteins of ion channels.

ICln is a protein that was identified by screening a cDNA library from Madin-Darby canine kidney (MDCK)[1] cells in *Xenopus laevis* oocytes using the two-electrode voltage-clamp technique (1). The expression of ICln in *X. laevis* oocytes results in an outwardly rectifying ion current that can be blocked by DIDS, 5-nitro-2-(3-phenylpropylamino)benzoic acid, and the addition of nucleotides to the extracellular fluid. The kinetic, selectivity, and pharmacology of the ICln-induced currents resemble those of the anionic currents activated after cell swelling in a variety of cells (2). The activation of these channels permits the exit of ions, which in turn leads to the exit of water, therefore allowing an effective regulatory volume decrease (3). The molecular entity of the regulatory volume decrease-induced "anionic" channels (RVDCs) is still elusive. Our hypothesis that ICln is a candidate for RVDCs is supported by the fact that the selective knockdown of the ICln protein in fibroblasts and epithelial cells leads to a substantial decrease in swelling-induced RVDC activation (4, 5). Furthermore, the nucleotide sensitivity of ICln expressed in oocytes was also found for RVDCs (5, 6), again demonstrating that ICln and RVDCs are closely related. Heterolog expression experiments were not able to unambiguously prove the channel nature of ICln, especially because we demonstrated that the ICln protein, despite its localization in the membrane, can also be identified (water-soluble) in the cytosol of growing cells. The successful reconstitution of the ICln ion channel in black lipid bilayers proved the channel nature of ICln; and the hypothesis that the water-soluble ICln protein could be directly transposed from the cytosol into the bilayer membrane, a mechanism that is well established for bacterial toxin channels (7–9), but so far unique for channel proteins in eukaryotic cells, was also proven by the very same approach. The reconstitution of ICln in bilayers furthermore allowed us to establish the binding site for the nucleotides on the ICln molecule and therefore to explain the nucleotide-induced block of the ICln current at a molecular level. The putative model of ICln is composed of two antipar-

The nucleotide sequence(s) reported in this paper has been submitted to the GenBank™/EBI Data Bank with accession number(s) AF202929–AF202932.

§ These authors contributed equally to this work.
¶ Present address: Kantonspital St. Gallen, Rorschacherstraße, CH-9007 St. Gallen, Switzerland.
‡‡ To whom correspondence should be addressed: Inst. für Physiologie und Balneologie, Fritz-Pregl-Str. 3, A-6020 Innsbruck, Austria. Tel.: 43-512-507-3756; Fax: 43-512-577656; E-mail: markus.paulmichl@uibk.ac.at or markus.paulmichl@unimi.it.

[1] The abbreviations used are: MDCK, Madin-Darby canine kidney; DIDS, 4,4′-diisothiocyanostilbene-2,2′-disulfonic acid; RVDC, regulatory volume decrease-induced anionic channel; RT, reverse transcription; ORF, open reading frame; RACE, rapid amplification of cDNA ends; GFP, green fluorescent protein; EGFP, enhanced green fluorescent protein; IRES, internal ribosome entry site; aa, amino acid(s).

allel β-sheets revealed a nucleotide-binding motif at the predicted extracellular vestibulum of the pore. Mutation of this motif was indeed followed by a block of the inhibitory effect of nucleotides on the induced current in oocytes (1) as well as after reconstitution of the mutant ICln proteins in a lipid bilayer (7). The ion selectivity of reconstituted ICln channel proteins seemed to argue against our hypothesis that ICln is the molecular entity of RVDCs (7, 10). However, the reconstitution of ICln in a mixture of heart lipids (11) instead of 1,2-diphytanoyl-*sn*-glycero-3-phosphocholine, an artificial lipid commonly used for artificial bilayers (7), indeed revealed the anionic selectivity of ICln, underscoring its prime role as the molecular RVDC candidate.

Besides the channel nature of the ICln protein, other functions of ICln that are not directly related to ion permeation seem to be feasible (10, 12). Sm proteins able to bind the ICln protein were identified using the yeast two-hybrid system (13, 14). Because it is obvious that the ICln protein can bind to an array of different proteins (14), we were interested in the identification of proteins that are able to functionally interact with the specific channel function of ICln. For this reason, we hoped to utilized the particular genome organization in the nematode *Caenorhabditis elegans*. In this organism, some genes are organized in operons. The genes in the same operon are transcribed together and controlled by a common promoter, and the assumption can be made that the products of these different genes are functionally linked. Therefore, we set out to clone the *C. elegans* homolog of ICln and to define whether or not the ICln gene is embedded in an operon. Our experiments revealed two splice variants of the ICln ion channel protein and the presence of an operon in which the ICln gene is embedded. Besides the ICln proteins termed IClnN1 and IClnN2, two additional proteins termed Nx and Ny were identified as part of the same operon. The functional reconstitution of the two splice variants of ICln in black lipid bilayers revealed (i) a current (IClnN1) similar to the current obtained after reconstitution of the MDCK homolog of ICln (7) and (ii) a current (IClnN2) characterized by a marked voltage-dependent inactivation at positive potentials. The molecular entity responsible for the inactivation was identified as a positively charged cluster of amino acids encoded by exon 2a, which is missing in IClnN1. The mechanism for the channel inactivation seems to be similar to the "ball and chain: mechanism responsible for the voltage-dependent inactivation of the *Shaker* potassium channels. The functional co-reconstitution of IClnN2 and Nx, one of the proteins encoded by the common operon, leads to a marked reduction of the voltage-dependent inactivation, thus demonstrating the functional interaction of the two proteins. This underscores the fact that the special genomic structure of the nematode genome allows the identification of functional partner proteins for ion channels.

EXPERIMENTAL PROCEDURES

Nematodes

The nematode strain (N2) used in this work was provided by the *Caenorhabditis* Genetics Center. The nematodes were grown on *Escherichia coli* strain OP50, harvested, and homogenized, and mRNA and genomic DNA were isolated according to standard protocols (15).

PCR Amplification

Standard PCR protocols with *Taq* or *Pfu* polymerase (Roche Molecular Biochemicals and Stratagene) were applied (15).

RT-PCR

RT-PCR was performed according to standard protocols (15) using avian myeloblastosis virus reverse transcriptase (Promega).

Identification of the Nematode ICln ORF—To increase the specificity of the RT-PCR, we used a modified poly(T) primer with an additional GC-rich tail sequence and G, A, or C at the 3′-end (5′-GCA TCG ATC GCG CGA CTC TTT TTT TTT TTT TTT TT(A/G/C)-3′, termed "poly(T) hook primer"). Using this primer, we performed reverse transcription of nematode mRNA, and this reaction was followed by two additional PCRs. In the first reaction, we used a primer starting at the predicted first ATG codon (5′-ATG ATT CTC ACT GAA GTC AGC C-3′) and a second primer complementary to the GC-rich hook sequence attached to the poly(T) sequence. In the second PCR step, the primer starting at the first ATG codon (see above) and a primer placed in the fourth exon of nematode ICln (5′-CCA TTT CCT CTT CTT CGT CGT CAT AC-3′) were used. The different PCR products were subcloned and sequenced thereafter.

Identification of the Nx and Ny ORFs—For this purpose, the first strand cDNA was synthesized using the poly(T) hook primer described above, followed by two PCRs specific for *Nx* or *Ny*. For *Nx*, the two primers used for the second PCR were 5′-ATG GCT CGT GGT CAA CAA AAG ATC-3′ and 5′-TCA AAG CTT CAA CGA GTT CTG CTG-3′. For *Ny*, the respective primers were 5′-ATG GCA ATG AAA ACC TTT CAG CAA AAA AC-3′ and 5′-ACG ACG TGG AAT TGG AGC AG-3′. Both PCR products were subcloned and sequenced.

5′-RACE

The first strand cDNA was made using avian myeloblastosis virus reverse transcriptase. The reaction was heat-inactivated and subjected to RNase A treatment. Unincorporated nucleotides and enzymes were removed using a QIAquick PCR purification column (QIAGEN Inc.). Where indicated, polyadenosine tails were added to the 5′-end using terminal deoxynucleotidyltransferase (MBI, Inc.). Second strand synthesis was carried out by PCR using *Taq* polymerase (MBI, Inc.) and the respective primers. To enhance the specificity of the PCR approach, the PCR products were usually subjected to a second "nested" PCR amplification.

Identification of the 5′-Untranslated Regions of Nx and Ny—For *Nx*, the first strand cDNA was synthesized using a primer with the sequence 5′-TCA AAG CTT CAA CGA GTT CTG CTG-3′. After the addition of a poly(A) tail to the 3′-end of the newly synthesized cDNA, a nested PCR was performed using the poly(T) hook primer in the forward direction and the 5′-TCA AAG CTT CAA CGA GTT CTG CTG-3′ primer in the reverse direction. For the second PCR (nested PCR), the GC-rich sequence of the forward primer was used together with a second reverse primer (5′-TGG GCT CTT TGG GTG CTT GTT C-3′). For *Ny*, the sequence-specific primer used for the first strand cDNA synthesis and for the first PCR was 5′-ACG ACG TGG AAT TGG AGC AG-3′, and that used for the second PCR was 5′-CAA TTG GTT TCG TAT GCT CGT ATG G-3′. The same primers for the *Nx* RACE were used as forward primers (see above).

Sequencing

All PCR products were sequenced using an automatic sequencer (LiCor Gene ReadIR 4200) with the protocols suggested by the manufacturer.

GFP Reporter Vector for IClnN1 Expression in NIH 3T3 Fibroblasts

Cloning Procedure—The bicistronic expression vector pIRES2-EGFP (CLONTECH) was used for transient transfection. This vector contains an MCS site, the cytomegalovirus promoter, the IRES sequence, and EGFP for positive selection of transfected cells. The *IClnN1* gene was cut out of the pET3-His vector (kindly provided by T. Hai, Ohio State University) (16) with *Xho*I and *Bam*HI, extracted from the gel, subcloned into pIRES2-EGFP, and sequenced. The IClnN1/IRES/EGFP vector construct was purified by conventional techniques and used for transient transfection.

Transient Transfection—The IClnN1/IRES/EGFP expression vector was transfected into NIH 3T3 fibroblasts using a method described previously (5). Briefly, NIH 3T3 cells (passages 40–100) were seeded the day before transfection (70,000 cells/3.5-cm Petri dish) and grown overnight. On the day of transfection, a mixture of 15 μl of Lipofectamine (Invitrogen) was diluted in 300 μl of serum-free Dulbecco's modified Eagle's medium (Sigma); 4 μg of plasmid DNA was added, followed by careful mixing. After 10–15 min at room temperature (20–25 °C), this mixture was overlaid onto 1 ml of serum-free Dulbecco's modified Eagle's medium in the Petri dish, and the cells were incubated for 6–10 h. Thereafter, cells were either detached and reseeded on glass coverslips for the experimental procedure on the next day (24 h) or fed 2 ml of 10% Dulbecco's modified Eagle's medium, detached after 24 h, and reseeded for experiments on the second day (48 h). The transfection rate was usually 20–30%.
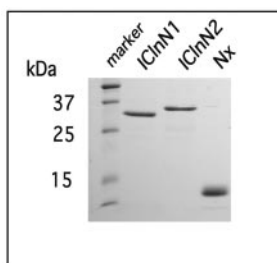
FIG. 1. **Purification of the IClnN1, IClnN2, and Nx proteins.** The ICln and Nx proteins were overexpressed and purified as described under "Experimental Procedures." The Coomassie Blue stain of the respective eluates shows bands of the expected sizes on 12% SDS-polyacrylamide gel.

Cell Culture—NIH 3T3 fibroblasts were grown in Dulbecco's modified Eagle's medium supplemented with 44 mM NaHCO$_3$, 280 μM penicillin, 114 μM streptomycin, and 10% fetal calf serum (5).

Fluorescence Microscopy—An Olympus OSP3-IMT2 microscope equipped with a xenon arc lamp was used to detect transfected cells expressing EGFP or cells loaded with dextran fluorescein. The dyes were excited at 488 nm, and emission was detected at 507 nm.

Functional Reconstitution of Nematode IClnN1, IClnN2, and Nx

Protein Purification—The ORFs of *IClnN1*, *IClnN2*, and *Nx* were cloned in frame into the pET3-His vector, adding a histidine tag to the N terminus of the respective proteins. The His tag allows purification of the different proteins on an Ni^{2+}-nitrilotriacetic acid-agarose column (QIAGEN Inc.). As shown in Fig. 1, overexpression of IClnN1, IClnN2, and Nx in *E. coli* strain BL21(DE3) (and their subsequent purification) led to protein bands of the expected sizes. The purified proteins were stored at −74 °C in elution buffer (50 mM K$_2$HPO$_4$ and 200 mM imidazole, pH 7.4–8.0) at a concentration of ≈0.1 μg/μl. To express the Nx protein in bacteria, a codon optimization had to be performed. For this, the codon for R22 was changed from AGA to CGT, and that for G25 was changed from GGA to GGT.

Bilayer Experiments

Macroscopic Currents—The experimental procedure used for the "black" lipid bilayer experiments is described in detail elsewhere (7, 17). The lipid bilayer was painted on an aperture of 1-mm diameter in a Teflon diaphragm separating the *cis*- and *trans*-chambers, each holding 5 ml of aqueous solution (100 mM KCl and 5 mM HEPES, pH 7.4). For the lipid bilayer membrane, 1% (w/v) 1,2-diphytanoyl-*sn*-glycero-3-phosphocholine (Avanti Polar Lipids) in *n*-decane and butanol was employed. After the membrane had turned optically black in the reflected light, the protein was added to the *cis*- and *trans*-chambers. All experiments were performed at room temperature. The membrane current was measured by a pair of Ag/AgCl reference electrodes (Metrohm) connected in series with a voltage source (*cis*) and a "current to voltage converter" (*trans*), which was made using a Burr Brown operational amplifier (9407/0541F). The signal was recorded with a strip chart recorder (BBC, Inc.).

Relative Selectivity of Reconstituted Nematode ICln—To determine the ion selectivity of reconstituted ICln, a gradient for the ions was established (*trans*: 150 mM KCl and 5 mM HEPES, pH 7.4; *cis*: 10 mM KCl and 5 mM HEPES pH 7.4). Because the establishment of the bilayer membrane requires time (during this period, the concentration gradient becomes reduced in both chambers, communicating through the circular hole (area of 0.8 mm^2)), the chloride gradient (ΔPD_{Cl}) was measured after each experiment using chloride-selective electrodes before the membrane was disrupted (7). The ΔPD_{Cl} value of every single experiment was used to calculate the pK/pCl value according to the Goldman-Hodgkin-Katz equation (18). The respective reversal potentials were determined graphically by interpolation.

Single Channel Currents—For the tip-dip experiments, the planar lipid bilayer was established on patch pipettes (7, 19). 1,2-Diphytanoyl-*sn*-glycero-3-phosphocholine was dissolved in *n*-decane for membrane formation. All measurements were performed in symmetrical KCl solutions (pipette and bath: 300 mM KCl and 10 mM HEPES, pH 7.4). The protein was added only to the bath solution. Single channel and whole cell currents were measured using a patch-clamp amplifier (HEKA) and Axopatch 200A (Axon Instruments, Inc.)), and the data were stored on tape or hard disc (20). For analysis, the data were filtered at 0.2 kHz. All experiments were performed at room temperature.

Whole Cell Patch-clamp Experiments—The procedures for whole cell patch-clamp experiments with NIH 3T3 fibroblasts and data analysis are described in detail by Gschwentner *et al.* (5). The control bath solution contained 125 mM NaCl, 2.5 mM MgCl$_2$, 2.5 mM CaCl$_2$, 100 mM mannitol, and 10 mM HEPES (adjusted with NaOH), pH 7.2. The hypotonic symmetrical solution contained 125 mM NaCl, 2.5 mM MgCl$_2$, 2.5 mM CaCl$_2$, and 10 mM HEPES (adjusted with NaOH), pH 7.2. The pipette solution contained 125 mM CsCl, 5 mM MgCl$_2$, 50 mM raffinose, 11 mM EGTA, 2 mM MgATP, and 10 mM HEPES (adjusted with CsOH), pH 7.2. The different peptides were added to the pipette solution at a final concentration of 3.4 μM. The diffusion of the peptide was controlled in a separate set of experiments using dextran fluorescein (M_r 3000; Molecular Probes, Inc.) added to the pipette at a final concentration of 10 μM. Of 65 cells tested, 59 cells showed a bright and 6 cells showed a lower fluorescence when tested within the same time frame of 5 min, used to determine the effect of peptides 1, 2, and 4. The holding potential in the different experiments was −60 mV, and voltage steps from −120 to +100 mV were performed (increments of +20 mV for 500 ms) under control as well as hypotonic conditions. To test the effect of the peptides, repetitive voltage steps were performed from a holding potential of −60 mV to +40 mV every 20 s.

Salts, Chemicals, and Drugs—All salts, chemicals, and drugs used were "pro-analysis" grade.

Statistical Analysis

All values are given as means ± S.E. Data were tested for differences in the means by Student's *t* test. A statistically significant difference was assumed at $p \leq 0.05$.

RESULTS

Chromosomal Localization of Nematode ICln

The genome of *C. elegans* has been fully sequenced (21)[2]; therefore, genes of interest can be identified by computer-aided sequence analysis. Using the N-terminal ICln amino acid sequence from zebrafish (*Brachydanio rerio*) (22), a Blast search[3] was performed, revealing similarity to a sequence from *C. elegans* that forms part of a cosmid clone (GenBank^{TM}/EBI Data Bank accession number Z68213). This cosmid clone is termed C01F6 and bears the *fem-3* locus of chromosome 4. Sequence analysis revealed that, in this cosmid clone, only part of the sequence coding for ICln is present. The remaining genomic sequence can be identified on the "downstream" cosmid clone of the same chromosome 4, *i.e.* ZC410 (accession number Z68270). The low homology among the C-terminal amino acid sequences of all ICln homologs cloned so far made it impossible to unambiguously define the exact ORF coding for nematode ICln by using simple sequence analysis.
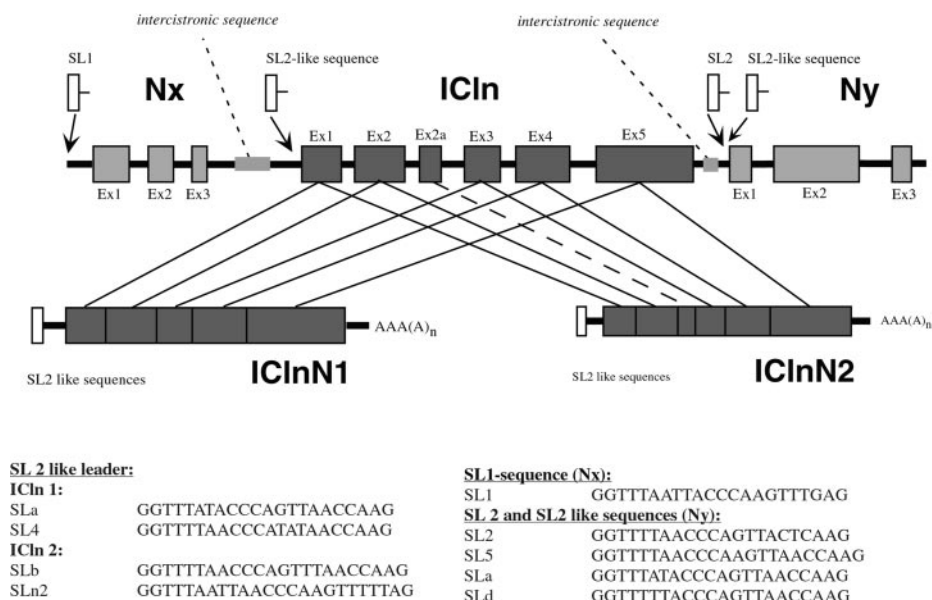
Identification of the ORF Coding for Nematode ICln

RT-PCR using *C. elegans* mRNA was performed to define the ORF coding for ICln. RT-PCR and nested PCR using the primer described under "Identification of the Nematode ICln ORF" should reveal a DNA fragment of 451 bp. However, we obtained two fragments of different sizes: one of 511 bp and a second, as expected, of 451 bp. This experiment unveiled the possibility that, in nematodes, two splice variants of ICln mRNA could be expressed, which was surprising because no other organism is known so far to exhibit splice variants of the ICln gene. After subcloning both fragments, the respective cDNAs were sequenced and indeed revealed the expected splice variants of the ICln mRNA. The entire ORFs of both splice variants were subsequently determined by additional PCR steps. The ORF of one splice variant is composed of 618 bp and codes for a protein of 205 amino acids (aa), termed *IClnN1* (GenBank^{TM}/EBI Data Bank accession number AF202931) (Fig. 2). The ORF of the second splice variant is composed of 678 bp and codes for a protein of 225 aa (accession number AF202932) (Fig. 2), termed *IClnN2*. The

FIG. 2. **ICln amino acid sequences from different species, including IClnN1 and IClnN2.** The four putative transmembrane segments are *boxed* and marked *I–IV* (first transmembrane domain of IClnN1 and IClnN2, DSLGNGTLYIT; second domain, SAAGTKGFSVAY; third domain, PAIVLHAIST; and fourth domain, HIFVMVDQRKS). The additional string of 20 aa encoded by exon 2a of IClnN2 is *underlined*. The position of the additional 20 aa is adjacent to the fourth putative transmembrane domain and therefore located in close proximity to the putative inner mouth of the pore.

coding region of *IClnN1* is composed of five exons (Fig. 3, *Ex1–5*). The second splice variant (*IClnN2*) is characterized by an additional exon (exon 2a) located between exons 2 and 3 (Fig. 3, *Ex2a*), which consists of 60 bp coding for a string of 20 aa with the sequence VRRRRRAPVLRTIQEDDEQR (Fig. 2). The amino acid sequence of IClnN1 is homologous to the ICln sequences identified in different species, *e.g.* human (accession number U17899; 54% similarity), dog (accession number X65450; 54% similarity), rabbit (accession number D26076; 54% similarity), rat (accession number D13985/L26450; 54% similarity), *X. laevis* (accession number L26449; 52% similarity), and zebrafish (accession number Y08484; 51% similarity). The additional amino acid string

encoded by exon 2a is unique for the nematode IClnN2 sequence and cannot be found in the ICln homologs of all other organisms tested so far. It is notable, however, that the first 10 aa determined by exon 2a are 70% homologous to a sequence (ARRRR-RGPVA) of the voltage-dependent calcium channel BI-2 (accession number X57477), a splice variant of the rabbit BI calcium channel (23).

Identification of the mRNAs Coding for IClnN1 and IClnN2

After identifying the two alternative ORFs coding for nematode ICln, we set out to test whether or not the ICln gene in nematodes is organized in an operon. Analysis of the 5′-ends of

FIG. 3. **Organization of the operon harboring IClnN1, IClnN2, Nx, and Ny and the SL sequences leading the respective RNAs.** The ICln gene in the nematode genome is embedded in an operon. The polycistronic mRNA deduced from this operon and identified by RT-PCR is depicted and shows the intron/exon structure of *IClnN1*, *IClnN2*, *Nx*, and *Ny*. *trans*-Splicing leads to the attachment of SL2-like sequences on the IClnN1 and IClnN2 mRNAs during mRNA maturation. The SL2-like sequences are given and marked accordingly. The ORFs of *Nx* and *Ny* are composed of three exons. An SL1 sequence can be identified leading the Nx RNA. The Ny RNA is led by SL2 or SL2-like sequences, which are given in detail. *Ex*, exon.

SL 2 like leader:

ICln 1:	
SLa	GGTTTATACCCAGTTAACCAAG
SL4	GGTTTTAACCCATATAACCAAG
ICln 2:	
SLb	GGTTTTAACCCAGTTTAACCAAG
SLn2	GGTTTAATTAACCCAAGTTTTTAG

SL1-sequence (Nx):

SL1	GGTTTAATTACCCAAGTTTGAG

SL 2 and SL2 like sequences (Ny):

SL2	GGTTTTAACCCAGTTACTCAAG
SL5	GGTTTTAACCCAAGTTAACCAAG
SLa	GGTTTATACCCAGTTAACCAAG
SLd	GGTTTTTACCCAGTTAACCAAG

the respective ICln RNAs should give the first clue because monocistronic RNAs derived from polycistronic RNA are led by SL1 or SL2 sequences. Using 5′-RACE, the 5′-untranslated regions of the two ICln mRNAs were determined. As shown in Fig. 3, SL2-like sequences were identified on the IClnN1 as well as IClnN2 mRNAs. These are short sequences that are not encoded by the same gene, but are *trans*-spliced during mRNA "maturation" (24). SL2 and SL2-like sequences can usually be found on those monocistronic RNAs encoded by genes that do not lead the operon (25). SL1 and SL1-like sequences can usually be found on the transcripts of the leading genes (26). Because these *trans*-spliced sequences were detected on neither IClnN1 nor IClnN2, it is reasonable to assume that the mRNA encoded by the ICln gene in nematodes might form part of a larger polycistronic pre-mRNA. Whereas the two known SL2-like sequences SLa and SL4 have been identified on the IClnN1 mRNA (27, 28), on the IClnN2 mRNA, in addition to the known SL2-like sequence SLb (27, 28), a new SL2-like sequence was found, which we termed SLn2 (Fig. 3). This SL sequence seems to be composed of two parts (SL-*bipartita*). Both nucleotide clusters, the first consisting of 11 or 12 nucleotides (GGTTTAATTAA/C-) and the second consisting of 12 or 13 nucleotides (-C/CCAAGTTTTTAG), can be found independently on multiple sites of the *C. elegans* genome. The mechanism by which the two clusters combine seems to be *trans*-splicing, the very same mechanism that leads thereafter to the grouping of the final SLn2 sequence and the IClnN2 mRNA.

Identification of the Operon Harboring the ICln Gene

Gene clusters of putative operons in *C. elegans* can be predicted because their genome is fully sequenced, and the transcription of these putative gene clusters can be tested. Analysis of the genomic sequence upstream and downstream of the ICln gene led to the identification of two ORFs coding for two putative proteins. We termed the upstream ORF and the derived protein Nx, and the ORF and protein encoded by the downstream gene Ny. To test the transcription of *Nx* and *Ny* and to further test if both mRNAs are linked in a polycistronic complex with ICln, we performed a set of RT-PCRs as described under "Experimental Procedures." The analysis revealed that the *Nx* ORF has a length of 222 bp (GenBank™/EBI Data Bank accession number AF202929) and consists of three exons and that the *Ny* ORF has a length of 330 bp (accession number AF202930) and consists also of three exons. To verify the 5′-

ends of the *Nx* and *Ny* ORFs, 5′-RACE was performed. These experiments confirmed the ORFs for *Nx* and *Ny*. In addition, these experiments revealed the SL sequences attached to the respective mRNAs. As shown in Fig. 3, the only SL sequence identified on Nx was SL1, and the sequences identified on Ny were the known SL2 sequence and three additional SL2-like sequences, excluding *Ny* as being the leading gene of the operon. In contrast, only SL1 sequences were identified on Nx, making it highly probable that *Nx* is in fact the leading gene of the operon. Because the processing of polycistronic RNA to monocistronic RNAs occurs after *cis*-splicing (intron elimination) of the pre-mRNA, RT-PCR and 5′-RACE can be used to identify the polycistronic RNA of the operon. A product was obtained and subcloned by performing reverse transcription by extending a primer complementary to a sequence starting at position +258 of the ICln gene (+1 is the A residue of the first codon), followed by adding a poly(A) tail to the 3′-end of the first strand cDNA and performing the first PCR step using the same reverse primer and the poly(T) hook primer. Subsequently, the plasmid containing the PCR product was subjected to a second PCR step using the GC-rich hook as the forward primer and a reverse complementary sequence specific to Nx as the reverse primer. This reaction gave rise to a cDNA product, which (after sequencing) revealed the Nx sequence as expected after *cis*-splicing, thus demonstrating that *Nx* and *ICln* are linked in a common operon. Because no additional genes upstream of the *Nx* gene were identified by this procedure, it must be assumed that *Nx* is the first gene of the operon, which is further substantiated by the finding that only SL1 sequences were identified on Nx (Fig. 3). To define the 3′-end of the operon, RT-PCR was performed using mRNA and a primer complementary to a sequence in the second exon of Ny for reverse transcription. Two consecutive PCRs were performed. For the first PCR, the same primer as for the reverse transcription was used together with a second primer, located in exon 5 of the ICln gene. The second PCR was performed with two nested primers, and the product was subcloned and sequenced. Because intron 1 of Ny was not amplified, we can exclude genomic contamination of our RNA preparation. In the polycistronic mRNA, the coding region of ICln is combined with the coding region of Ny. We were not able to identify coding regions farther downstream of Ny using 3′-RACE. These experiments

Functional Characterization of Nematode ICln
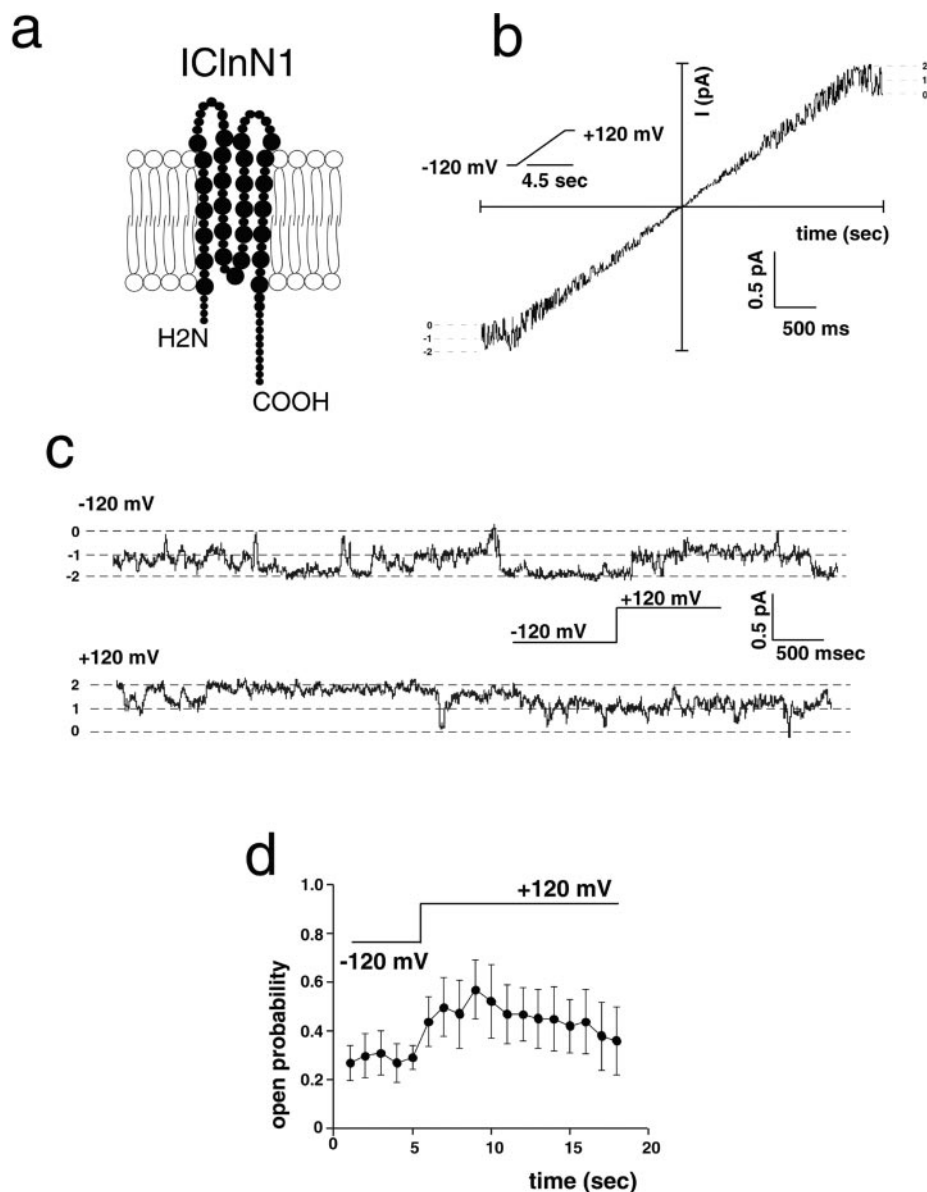
FIG. 4. **Single channel analysis of reconstituted IClnN1 channels.** *a*, the schematic visualizes the putative topology of one IClnN1 unit in the membrane. The putative model was made according the model of MDCK ICln (1). A continuous voltage ramp was applied to test for the voltage dependence of the induced currents. After holding the membrane for 500 ms at −120 mV, the voltage was continuously increased at a rate of 53.4 mV/s to +120 mV, and then the potential was held there for 500 ms. *b*, in the experiment shown, two channels (*1* and *2*; *0* = closed state) were present. *c*, an original recording of IClnN1 is shown at holding potentials of −120 and +120 mV. The P_o of the IClnN1 channels was determined from experiments such as shown in *c* at the two potentials indicated, at intervals of 1 s; and these values are summarized in *d*.

confirm that the polycistronic mRNA includes the ORFs of *Nx*, *ICln*, and *Ny* (Fig. 3).

Functional Reconstitution of the Two Splice Variants of ICln in Lipid Bilayers

Macroscopic Current Measurements—In the presence of symmetrical KCl concentrations (100 mM KCl at the *cis*- and *trans*-sides of the bilayer), purified IClnN1 or IClnN2 proteins were added to both sides of the bilayer, and the linear currents (evidenced by the rectification parameters $|I_{+50 \text{ mV}}/I_{-50 \text{ mV}}|$ of 1.11 ± 0.36 ($n = 5$) for IClnN1 and 0.94 ± 0.15 ($n = 4$) for IClnN2) obtained were not different from each other and from the current obtained after the reconstitution of MDCK ICln (7). To estimate the relative ion selectivity of IClnN1 or IClnN2, experiments were performed in the presence of a KCl gradient. Using a KCl gradient of 10/150 mM KCl (*cis/trans*), reversal potentials of $+24.09 \pm 2.6$ mV ($n = 24$) and $+25.48 \pm 3.8$ mV ($n = 11$) were measured for IClnN1 and IClnN2, respectively. According to the Goldman-Hodgkin-Katz equation (18), pK/pCl values of 8.12 ± 1.8 ($n = 24$) and 5.69 ± 1.2 ($n = 11$) were calculated for IClnN1 and IClnN2, respectively. As described earlier (7), single channel events cannot be resolved using large bilayer membranes. To perform single channel measurements

of IClnN1 and IClnN2, we incorporated the respective proteins in bilayers established on the tip of patch electrodes. This technique is referred to as "tip-dip" method and is described by Fürst *et al.* (7) (for details, see Refs. 19 and 29).

Single Channel Analysis of IClnN1—The reconstitution of IClnN1 in the tip-dip configuration was followed by the appearance of single channel currents (Fig. 4). It is important to mention that IClnN1 is the splice variant of ICln lacking the additional string of 20 aa and is therefore similar to the ICln homologs cloned from other species (Figs. 2 and 4*a*) (7, 22). The single channel conductance at −120 mV is 1.87 ± 0.22 picosiemens ($n = 8$), which is similarly low compared with the single channel conductance of ≈ 3 picosiemens obtained by reconstituting the MDCK homolog of IClnN1 (7). The open probability (P_o) of IClnN1 channels is independent of the holding potential. A voltage-clamp protocol was designed in which, after initially holding the membrane patch at −120 mV for 5 s, a voltage step to +120 mV was performed (Fig. 4, *c* and *d*). At +120 mV, the P_o was calculated for a period of 12 s. The calculated P_o values were 0.29 ± 0.07 ($n = 8$) at −120 mV and 0.41 ± 0.12 ($n = 7$) at +120 mV, values not statistically significantly different from each other. Similar P_o values were determined for MDCK ICln at +75 mV, *i.e.* 0.29 (7).
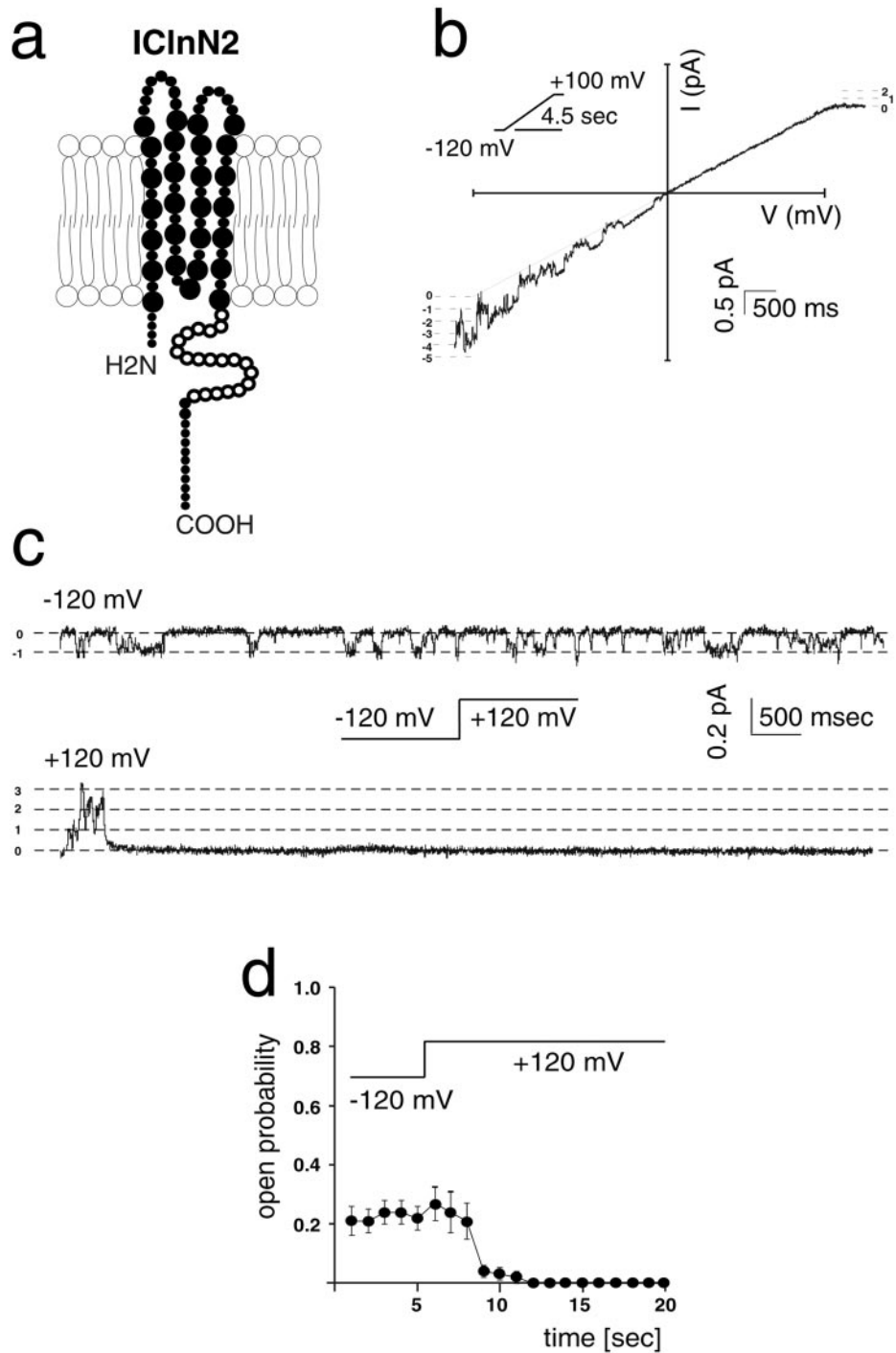
FIG. 5. **Single channel analysis of the reconstituted IClnN2 channels.** *a*, the IClnN2 protein is a splice variant of nematode ICln and is characterized by an additional string of 20 (*open circles*), which is located immediately after the predicted fourth transmembrane domain, in close proximity to the predicted inner mouth of the ion-conducting pore. *b*, a continuous voltage ramp was applied to test for the voltage dependence of the IClnN2-induced currents. After holding the membrane for 500 ms at −120 mV, the voltage was continuously increased at a rate of 48.9 mV/s to +100 mV, and then the potential was held there for 500 ms. In the experiment shown, five channels (*1–5; 0* = closed state) could be identified at −120 mV, whereas at positive potentials, these channels were inactivated. *c*, an original recording is shown at −120 and +120 mV, evidencing the voltage-dependent inactivation of the IClnN2-induced channels at positive potentials. The P_o of the IClnN2 channels was determined from experiments as shown in *c* at the two potentials indicated, in intervals of 1 s; and these values are summarized in *d*.

Single Channel Analysis of IClnN2—Identical experiments as described for IClnN1 were performed for IClnN2. The single channel conductance of IClnN2 was not statistically significantly different from that of IClnN1, *i.e.* 2.20 ± 0.20 picosiemens ($n = 13$). In contrast to IClnN1, the reconstituted IClnN2 channels showed a dramatic dependence of the P_o on the holding potential (Fig. 5, *c* and *d*). After a voltage step from −120 to +120 mV, the P_o dropped from 0.22 ± 0.04 ($n = 13$) to close to zero (0.01 ± 0.01, $n = 13$).

The IClnN1 Current Can Be Converted into the IClnN2 Phenotype by Adding Peptides Encoded by Exon 2a—The addition of peptide 1, which is composed of the same amino acids as the amino acid string encoded by exon 2a, to reconstituted IClnN1 led to a similar current phenotype as obtained by the reconstitution of the IClnN2 channel protein. Whereas, in the absence

of the peptide, the voltage step from −120 to +120 mV was not followed by a change in the P_o, in the presence of peptide 1, the P_o was dramatically reduced at −120 mV as well as at +120 mV (Figs. 6*b* and 7*a*). Analysis of the amino acids of peptide 1 revealed two sections, one with a net positive charge and a second with a net negative charge (Fig. 6*a*). At a positive holding potential, the membrane side accessible from the bath was negatively charged (for experimental conditions, see "Experimental Procedures") and should therefore facilitate the approach of the positive charge to the pore entrance and hence favor inhibition. To test this hypothesis, we used three additional peptides, *i.e.* peptide 2, composed of the first 10 aa (predominantly positively charged amino acids) (Fig. 6*a*, *box* marked with +); peptide 3, composed of the subsequent 10 aa (predominantly negatively charged amino acids) (*box* marked
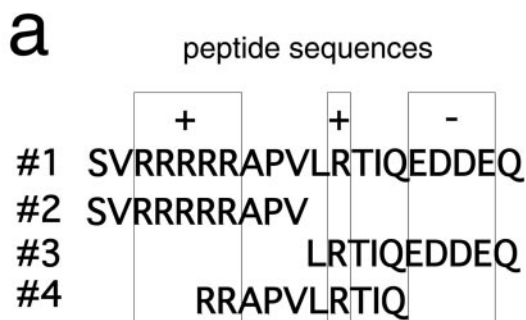
FIG. 6. **The 20-aa peptide encoded by exon 2a is able to transform the IClnN1 current.** The addition of the peptide with the sequence SVRRRRRAPVL-RTIQEDDEQ (peptide 1; shown in *a*) to reconstituted IClnN1 led to voltage-dependent inactivation similar to that observed after reconstituting IClnN2. Before the addition of the peptide, the P_o values of the IClnN1-induced channels were measured at −120 and +120 mV, respectively. Then 15 μg of the peptide was added, and the P_o was determined as in the absence of the peptide (*b*). A summary of these experiments is given in Fig. 7.
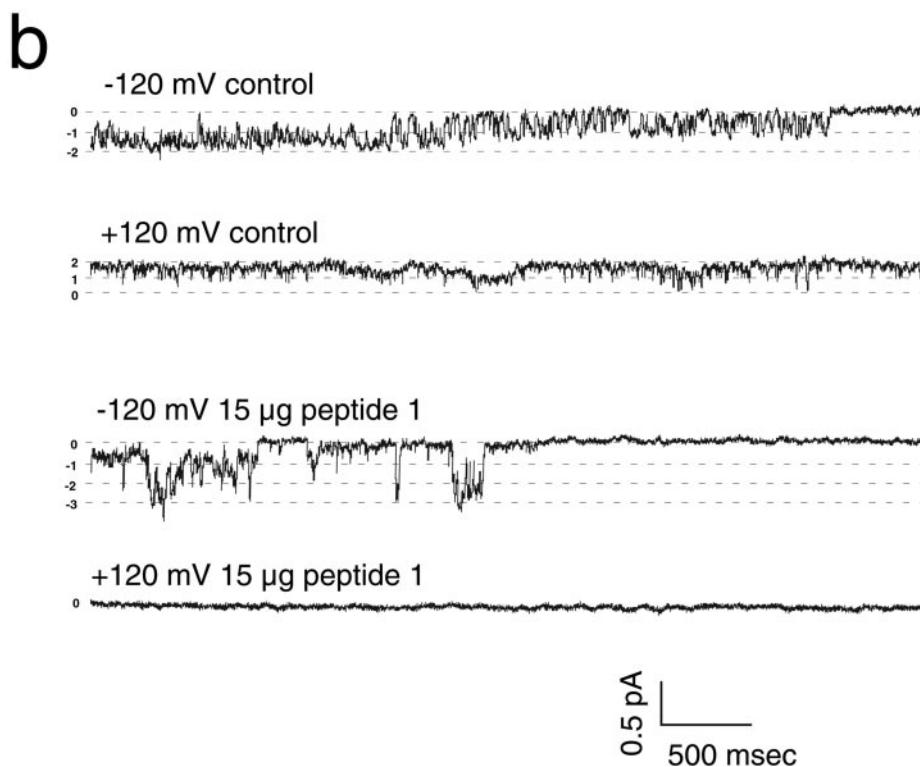
with −); and peptide 4, located between the two charged clusters. As depicted in Fig. 7, only peptides 1 and 2, both containing the positively charged cluster composed of five arginines, were able to reduce the current evoked by IClnN1 at −120 and +120 mV, respectively. Peptides 3 and 4 were both ineffective and did not lead to a reduced current, either at positive or negative holding potentials (Fig. 7, *c* and *d*).

Effect of the Exon 2a Peptides on Swelling-induced Ion Currents in Native Mouse Cells—As described previously, ICln is an important entity for the RVDCs (4, 5, 30, 31). Therefore, we set out to test whether or not the peptides used to characterize nematode ICln are functionally active on RVDCs in NIH 3T3 fibroblasts (2, 5, 6). Peptide 1 (1 μM) as well as peptide 2 (1 μM), which were both able to inactivate the IClnN1-induced current in bilayer experiments, were ineffective on ion currents in native fibroblasts under control conditions as well as after swelling of the cells (Fig. 8*a*). It is feasible to assume that in addition to the applied potential, also a molecular interaction between the positive cluster and the pore region has to occur to effect inactivation. Because IClnN1 and mouse ICln do not

have an identical amino acid sequence, we expressed IClnN1 in NIH 3T3 fibroblasts and then applied the respective peptides. Because, under these conditions, in addition to the endogenous mouse ICln channels, also the peptide-sensitive nematode IClnN1 channels are present in the same cell system, the peptides should allow the reduction of at least part of the swelling-induced currents.

Expression of IClnN1 in NIH 3T3 Fibroblasts—The expression of the IClnN1 protein in NIH 3T3 fibroblasts was verified by the simultaneous expression of modified GFP. Because the ORFs for *IClnN1* and *GFP* are located on the same vector, but separated by an IRES sequence, the simultaneous transcription of both ORFs can be expected, despite the fact that both proteins need not be fused (32). Only cells showing GFP fluorescence were tested (Fig. 8*b*, *inset*). Under control conditions, peptide 2 was without an effect, as in the absence of IClnN1 in these cells. However, after reducing the extracellular osmolarity by 100 mosM, an effect of peptide 2 could be observed at potentials of +80 mV or higher (Fig. 8*b*). This effect could be observed only when the peptide was added to the pipette solu-
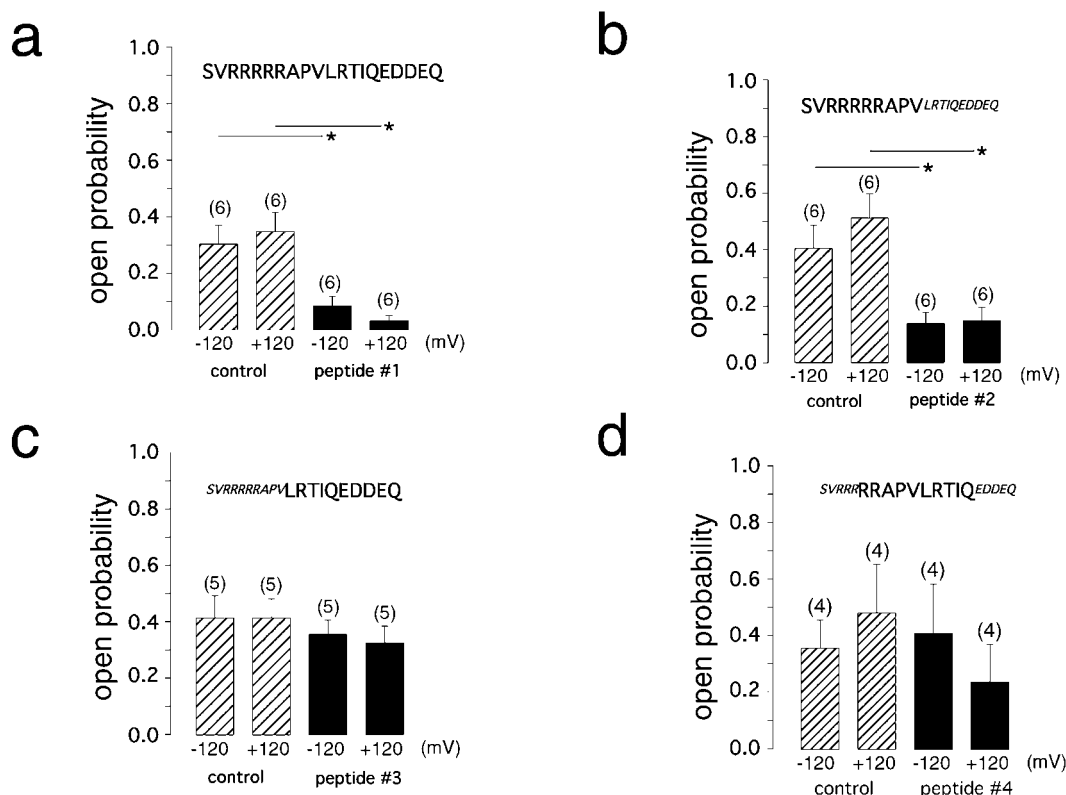
FIG. 7. **Effect of exon 2a peptides on the voltage-dependent inactivation of IClnN1.** *a*, as shown in Fig. 6, in the absence of peptide 1 (*control*), the reconstituted IClnN1 channels showed no voltage-dependent inactivation. However, in the presence of peptide 1 (see Fig. 6*b*), the current was reduced at negative as well as positive potentials. The P_o values in the absence of the peptide at -120 and $+120$ mV were 0.31 ± 0.07 ($n = 6$) and 0.35 ± 0.07 ($n = 6$), respectively. These values were significantly reduced for both potentials in the presence of peptide 1, *i.e.* 0.09 ± 0.03 ($n = 6$) and 0.03 ± 0.02 ($n = 6$), respectively. *b*, a reduction of the IClnN1-induced current could also be observed in the presence of peptide 2 (*large letters*, first 10 aa containing five arginines; *box* marked with + in Fig. 6*a*). For peptide 2, the P_o values were 0.41 ± 0.08 ($n = 6$) and 0.51 ± 0.09 ($n = 6$) at -120 and $+120$ mV, respectively, in the absence of the peptide; and both values were significantly reduced to 0.14 ± 0.08 ($n = 6$) and 0.15 ± 0.05 ($n = 6$), respectively, in the presence of the peptide. *c* and *d*, peptides 3 and 4 were ineffective and did not reduce the IClnN1-induced currents, either at negative or positive potentials (-120 and $+120$ mV): 0.42 ± 0.08 ($n = 5$) and 0.42 ± 0.07 ($n = 5$), respectively, in the absence of peptide 3; 0.36 ± 0.05 ($n = 5$) and 0.33 ± 0.06 ($n = 5$), respectively, in the presence of peptide 3; 0.36 ± 0.10 ($n = 4$) and 0.48 ± 0.17 ($n = 4$), respectively, in the absence of peptide 4; and 0.41 ± 0.18 ($n = 4$) and 0.24 ± 0.13 ($n = 4$), respectively, in the presence of peptide 4. The single channel conductances did not change in the presence of peptides 1–4 and varied between 1 and 3 picosiemens (data not shown).
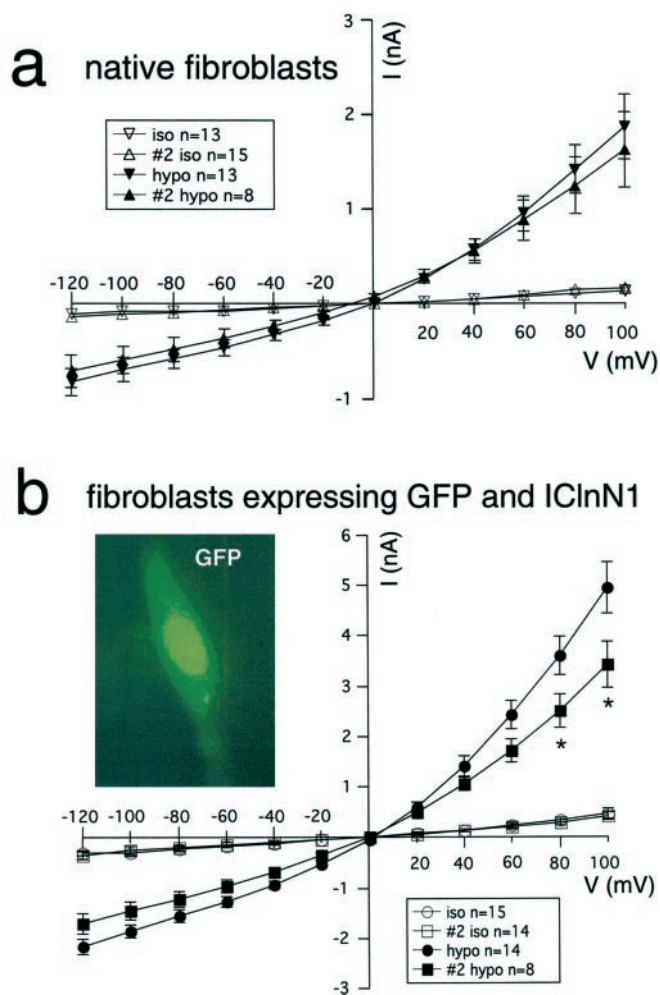
tion, allowing its diffusion into the cytosol to reach the cytoplasmic domains of the reconstituted IClnN1 channels. The addition of the peptide to the extracellular fluid did not affect the swelling-dependent ion current. It is important to note that the current elicited by swelling in cells expressing IClnN1 was higher compared with the currents measured in control cells (Fig. 8, *a* and *b*). Because the current in IClnN1-expressing cells under control conditions was indistinguishable from that in cells not expressing IClnN1, it can be assumed that IClnN1 channels are (like the endogenous RVDCs) not active under control conditions. However, reducing the extracellular osmolarity led to the activation of endogenous RVDCs, which were insensitive to peptide 2, as well as to the activation of the IClnN1 channels, which were sensitive to peptide 2 (Fig. 8*b*). To test the specificity of this approach, we performed control experiments using peptide 4, which proved to be ineffective on reconstituted IClnN1 channels, demonstrating the specificity of peptide 2.

Functional Interaction between IClnN2 and Nx—To test a possible functional interaction of the different gene members of the ICln operon in *C. elegans*, we tested the effect of the Nx protein after reconstituting the IClnN2 channels. The voltage-dependent inactivation at positive holding potentials observed after reconstitution of the IClnN2 splice variant could be markedly reduced in the presence of the Nx protein, as illustrated in Fig. 9. The decrease in the P_o observed after reconstituting IClnN2 was from 0.30 ± 0.06 ($n = 7$; -120 mV) to 0.06 ± 0.06

($n = 7$; $+120$ mV). Nx prevented the inactivation of the current at $+120$ mV (0.24 ± 0.05 ($n = 7$; -120 mV) and 0.20 ± 0.06 ($n = 7$; $+120$ mV)). This demonstrates that both proteins can interact on a functional level. An important finding is that, for the nematode Nx protein, a highly homologous (71%) human protein was identified by searching data bases and performing RT-PCR in HL-60 cells (forward primer, 5′-CGTGGACAGCA-GAAAATTCAG-3′; and reverse primer, 5′-AGTGGAGTCT-TAGGATGCTTG-3′). This protein is termed HSPC038 (Gen-Bank^{TM}/EBI Data Bank accession number AAD39916) because it was originally predicted from the cDNA of hematopoietic stem progenitor cells. The function of the HSPC038 protein is unknown. A human homolog was also identified for the Ny protein, albeit with a lower overall similarity (36%) (HSPC204; accession number AAF36124). The His-tagged version of Ny cannot be expressed in the bacterial expression system; and therefore, it was not possible to test a functional interaction of this protein with nematode ICln.

DISCUSSION

In *C. elegans*, two splice variants of the ICln gene are expressed. To functionally characterize the two splice variants of ICln, we reconstituted the proteins in black lipid bilayers. The sole addition of the purified proteins of IClnN1 or IClnN2 to the salt solutions of the bilayer set-up was followed by the appearance of ionic currents. This finding is in agreement with our previous results obtained after reconstituting MDCK ICln pro-

a native fibroblasts

- ▽ iso n=13
- △ #2 iso n=15
- ▼ hypo n=13
- ▲ #2 hypo n=8

b fibroblasts expressing GFP and IClnN1

GFP

- ○ iso n=15
- ⊟ #2 iso n=14
- ● hypo n=14
- ■ #2 hypo n=8

FIG. 8. **Effect of peptide 2 on NIH 3T3 fibroblasts expressing IClnN1.** Peptide 2, at a concentration of 1 μM, was ineffective on endogenous RVDCs in NIH 3T3 fibroblasts under control (isotonic (*iso*)) or hypotonic (*hypo*) conditions (*a*). However, after expression of IClnN1 in fibroblasts, a significant inhibition of the swelling-induced current at positive potentials ($\geq$80 mV) could be measured in the presence of peptide 2 (*b*). The *inset* depicts a fibroblast expressing GFP. These cells were selected for the current measurements because the GFP gene is combined by an IRES sequence with the *IClnN1* gene for expression.

teins in lipid bilayers (7). The present experiments again demonstrate that water-soluble ICln proteins can be inserted directly into the membrane and function as ion channels, a mechanism that is well established for bacterial toxins, but unique for ion channels in eucaryotic cells (9).

The functional reconstitution of IClnN1 and IClnN2 revealed two different current phenotypes. Whereas the P_o of IClnN1 channels is not dependent on the holding potential, the P_o of IClnN2 is dramatically reduced at positive potentials. As mentioned above, the IClnN2 splice variant of nematode ICln is characterized by the presence of an additional string of 20 aa in close vicinity to the inner vestibulum of the ion-conducting pore, as predicted by the putative ICln model (Fig. 5a). The voltage-dependent inactivation of IClnN2 could be explained on a molecular level assuming a functional similarity to the *Shaker* potassium channel. In 1990, Aldrich and co-workers (33, 34) proposed a ball and chain model for the voltage-dependent inactivation of *Shaker* potassium channels. In analogy, the additional string of amino acids encoded by exon 2a in IClnN2 could act as a mobile and charged "ball," leading to the observed inhibition of the channel activity at positive potentials. We tested this hypothesis by adding the 20 aa encoded by exon 2a of IClnN2 as a synthetic peptide to the current effected

-120 mV | +120 mV
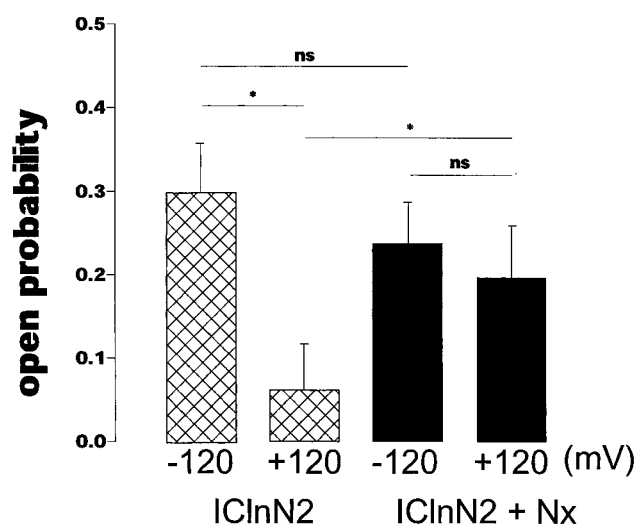
FIG. 9. **Functional interaction between IClnN2 and Nx in lipid bilayers.** The reconstitution of IClnN2 led to a current that inactivated at positive potentials (see also Fig. 5). If the Nx protein was added to the reconstituted IClnN2 channels, the voltage-dependent inactivation was no longer observed. *ns*, not significant.

by IClnN1, the splice variant lacking the 20-aa string and voltage-dependent inactivation. This procedure made the P_o of IClnN1 voltage-dependent, supporting our hypothesis that the string of 20 aa encoded by exon 2a of IClnN2 is responsible for the observed voltage-dependent decrease in the P_o.

The voltage-dependent inactivation of IClnN2 due to the amino acid string encoded by exon 2a seems to be species-specific. At low peptide concentrations, the anionic currents in mouse fibroblasts cannot be affected either under isotonic or hypotonic conditions. We investigated the effect of the peptide under hypotonic conditions because it is feasible to assume that ICln is a substantial part of the ion channel activated after cell swelling. In agreement with our hypothesis is the finding that, if IClnN1 is expressed in fibroblasts, cell swelling activates a larger current compared with cells not expressing IClnN1, and the peptide is indeed able to reduce a substantial part of the induced current. This supports our hypothesis that ICln is critically involved in volume regulation. The inability of the peptide to functionally interact with the native mouse channels could be explained by the substantial sequence differences between mouse and nematode ICln. Different peptide concentrations and/or mutation of the mouse ICln protein will help to elucidate the molecular mechanism of the peptide-induced inactivation.

The ICln gene in *C. elegans* is embedded in an operon, composed of two additional genes. We called the leading gene *Nx* (wormbase designation C01F6.9). The Ny protein is located downstream of ICln (wormbase designation ZC410.7b). A larger variant (eight exons) was also suggested for the Ny protein (wormbase designation ZC410.7a). However, we were not able to confirm the longer variant of Ny using 3'-RACE. This does not exclude, however, the possibility that, under conditions we have not tested, a longer version of Ny can be expressed. The co-reconstitution of ICln and *Nx*, the leading gene of the polycistronic RNA coding for ICln, revealed a functional interaction between both proteins. The physiological meaning of this interaction remains to be elucidated. However,

Maeda *et al.*[4] reported RNA_i experiments using the Nx (C01F6.9) as well as the Ny (ZC410.7a/b) sequences and found that knocking out the Nx protein is followed by a slow growth of the worms, whereas knocking out the Ny protein is lethal.[4]

In conclusion, the isolation of the polycistronic nematode RNAs coding for ion channels, as shown here, can serve as a strategy for identifying functional partner proteins for ion channels. Two different splice variants of ICln can be identified in the nematode *C. elegans*. Both splice variants (IClnN1 and IClnN2) can be functionally reconstituted in lipid bilayers, and the currents elicited by both channel proteins show distinct differences in voltage dependence. Whereas the IClnN1 currents show no voltage-dependent inactivation, the IClnN2 channels fully inactivate at positive potentials. The molecular entity responsible for the voltage-dependent inactivation was identified as a cluster of positively charged amino acids located in the amino acid string encoded by exon 2a of IClnN2, which is absent in IClnN1. However, IClnN1 channels are sensitive to peptides composed of the positively charged amino acid cluster, suggesting that this sequence could bend and therefore lead to the voltage-dependent inactivation observed for IClnN2 channels. In addition, the described functional interaction of IClnN2 and Nx (both proteins embedded within the same operon) indicates that the nematode might provide an effective approach for the identification of functional partner proteins of ion channels.

REFERENCES

1. Paulmichl, M., Li, Y., Wickmann, K., Ackerman, M., Peralta, E., and Clapham, D. (1992) *Nature* **356,** 238–241
2. Gschwentner, M., Susanna, A., Schmarda, A., Laich, A., Nagl, U. O., Ellemunter, H., Deetjen, P., Frick, J., and Paulmichl, M. (1996) *J. Allergy Clin. Immunol.* **98,** 98–101
3. Lang, F., Busch, G. L., Ritter, M., Volkl, H., Waldegger, S., Gulbins, E., and Haussinger, D. (1998) *Physiol. Rev.* **78,** 247–306
4. Chen, L., Wang, L., and Jacob, T. J. (1999) *Am. J. Physiol.* **276,** C182–C192
5. Gschwentner, M., Nagl, O. U., Wöll, E., Schmarda, A., Ritter, M., and Paulmichl, M. (1995) *Pfluegers Arch. Eur. J. Physiol.* **430,** 464–470
6. Gschwentner, M., Susanna, A., Wöll, E., Ritter, M., Nagl, U. O., Schmarda, A., Laich, A., Pinggera, G. M., Ellemunter, H., Huemer, H., Deetjen, P., and Paulmichl, M. (1995) *Mol. Med.* **1,** 407–417
7. Fürst, J., Bazzini, C., Jakab, M., Meyer, G., Konig, M., Gschwentner, M., Ritter, M., Schmarda, A., Bottà, G., Benz, R., Deetjen, P., and Paulmichl, M. (2000) *Pfluegers Arch. Eur. J. Physiol.* **440,** 100–115
8. Li, C., Breton, S., Morrison, R., Cannon, C. L., Emma, F., Sanchez-Olea, R., Bear, C., and Strange, K. (1998) *J. Gen. Physiol.* **112,** 727–736
9. Parker, M. W., Pattus, F., Tucker, A. D., and Tsernoglou, D. (1989) *Nature* **337,** 93–96
10. Clapham, D. E. (1998) *J. Gen. Physiol.* **111,** 623–624
11. Garavaglia, L., Bazzini, C., Bottà, G., Fürst, J., Gschwentner, M., Jakab, M., König, M., Meyer, G., Provenzano, J., Ritter, M., Rodighiero, S., and Paulmichl, M. (2002) *Pfluegers Arch. Eur. J. Physiol.*, in press
12. Gschwentner, M., Fürst, J., Schmarda, A., Bazzini, C., Wöll, E., Ritter, M., Dienstl, A., Scandella, E., Oehl, B., Hohlrieder, M., and Paulmichl, M. (1998) in *Cell Volume Regulation: The Molecular Mechanism and Volume Sensing Machinery* (Okada, Y., ed) Elsevier Science Publishers B. V., Amsterdam
13. Pu, W. T., Krapivinsky, G. B., Krapivinsky, L., and Clapham, D. E. (1999) *Mol. Cell. Biol.* **19,** 4113–4120
14. Schmarda, A., Fresser, M., Gschwentner, M., Fürst, J., Ritter, M., Lang, F., Baier, G., and Paulmichl, M. (2001) *Cell. Physiol. Biochem.* **11,** 55–60
15. Maniatis, T., Fritsch, E., and Sambrook, J. (1982) *Molecular Cloning: A Laboratory Manual*, Cold Spring Harbor Laboratory, Cold Spring Harbor, NY
16. Chen, B. P. C., and Hai, T. (1994) *Gene (Amst.)* **139,** 73–75
17. Benz, R., Maier, E., Thinnes, F. P., Götz, H., and Hilschmann, N. (1992) *Biol. Chem. Hoppe-Seyler* **373,** 295–303
18. Hille, B. (1992) *Ionic Channels of Excitable Membranes*, Sinauer Associates, Inc., Sunderland, MA
19. Ehrlich, B. (1992) *Methods Enzymol.* **207,** 463–470
20. Meyer, G. (1995) *Bioelectrochem. Bioenerg.* **36,** 23–31
21. The *C. elegans* Sequencing Consortium (1998) *Science* **282,** 2012–2018
22. Schmarda, A., Nagl, O., Gschwentner, M., Fürst, J., Hofer, S., Deetjen, P., and Paulmichl, M. (1997) *Cell. Physiol. Biochem.* **7,** 298–302
23. Mori, Y., Friedrich, M., Kim, A., Mikami, J., Nakai, P., Ruth, P., Bosse, E., Hofman, F., Flockerzi, V., Furuichi, T., Mikoshiba, K., Imoto, K., Tanaba, T., and Numa, S. (1991) *Nature* **350,** 398–402
24. Agabian, N. (1990) *Cell* **61,** 1157–1160
25. Spieth, J., Brooke, G., Kuersten, S., Lea, K., and Blumenthal, T. (1993) *Cell* **73,** 521–532
26. Blumenthal, T. (1998) *Bioessays* **20,** 480–487
27. Ferguson, C., and Rothman, H. (1999) *Mol. Cell. Biol.* **19,** 1892–1900
28. Ross, H., Freedman, H., and Rubin, S. (1995) *J. Biol. Chem.* **270,** 22066–22075
29. Coronado, R., and Latorre, R. (1983) *Biophys. J.* **43,** 231–236
30. Hubert, M. D., Levitan, I., Hoffman, M. M., Zraggen, M., Hofreiter, M. E., and Garber, S. S. (2000) *Biochim. Biophys. Acta* **1466,** 105–114
31. Tao, G. Z., Komatsuda, A., Miura, A. B., Kobayashi, A., Itoh, H., and Tashima, Y. (1998) *Biochem. Biophys. Res. Commun.* **247,** 668–673
32. Vagner, S., Waysbort, A., Marenda, M., Gensac, M., Amalric, F., and Prats, A. (1995) *J. Biol. Chem.* **270,** 20376–20383
33. Hoshi, T., Zagotta, W., and Aldrich, R. (1990) *Science* **250,** 533–538
34. Zagotta, W., Hoshi, T., and Aldrich, R. (1990) *Science* **250,** 568–571

---

[4] www.wormbase.org.